Jefferson Lab Users
Organization (JLUO) Annual
Meeting, 13-15 June 2022

Neutron Skin Measurement of ^{208}Pb Using Parity-Violating Electron Scattering

Devi L. Adhikari – June 14, 2022
Idaho State University (Currently at Virginia Tech)
for PREX-2 and CREX Collaborations

JSA PhD Thesis Prize Talk

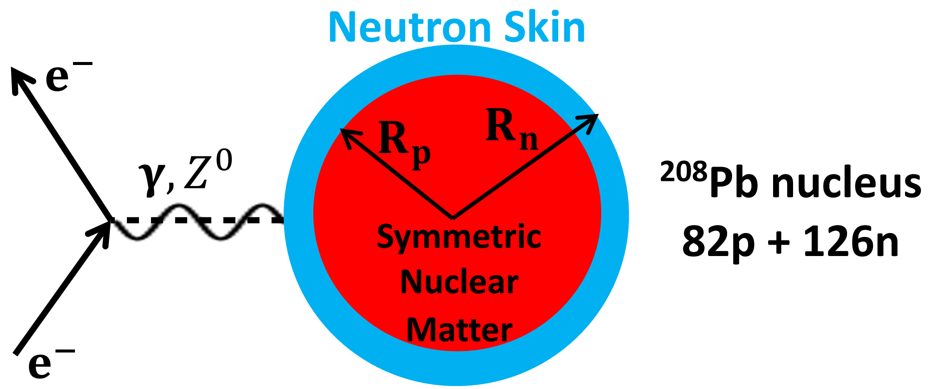

Outline

- Overview (parity, its non-conservation and PVES)
- Experimental components
- Parity-violating asymmetry and its precision
- Neutron skin extraction and its implications
- Summary

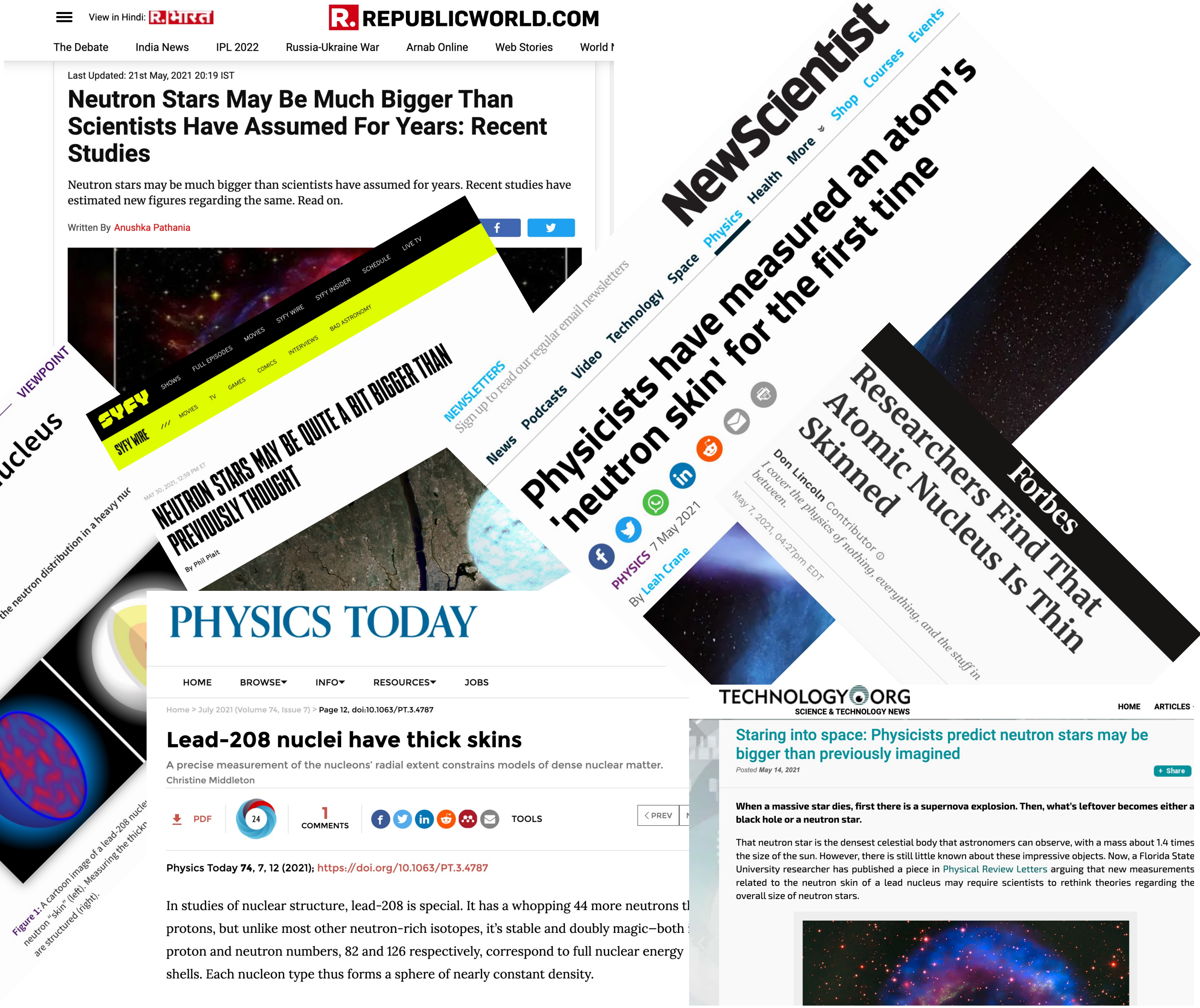

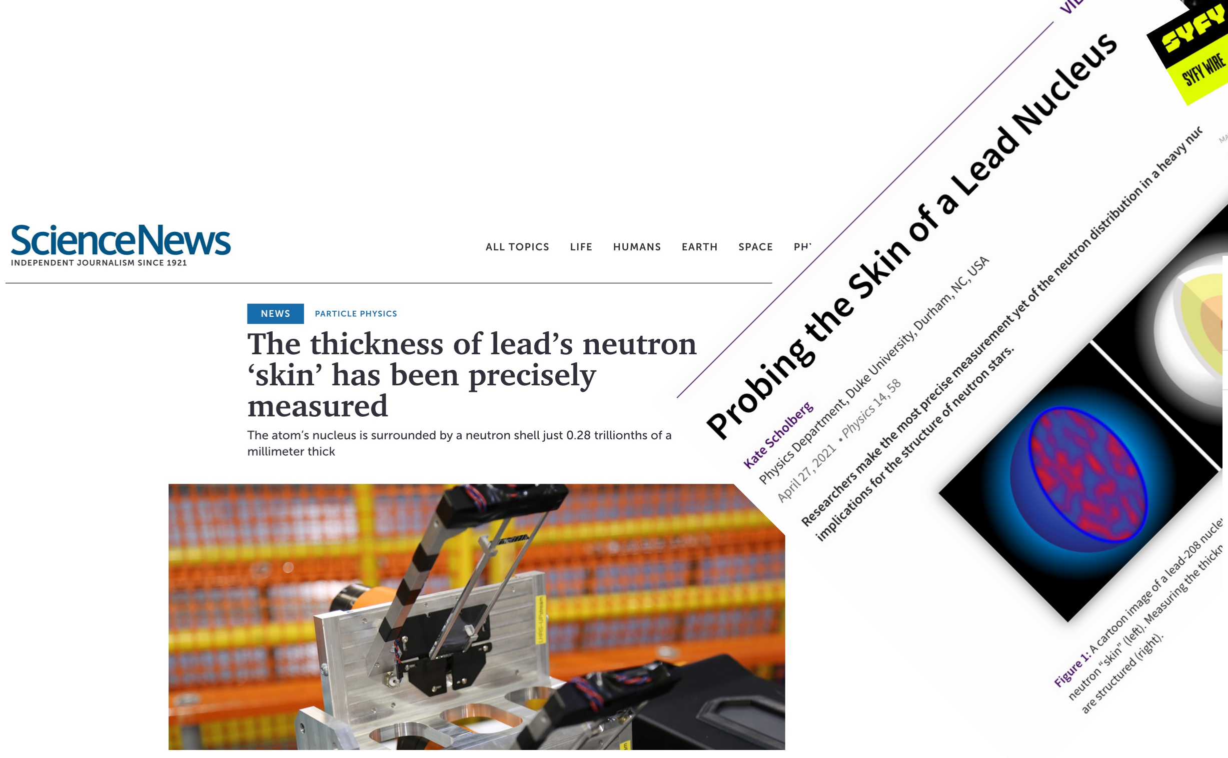

Overview

- PREX-2 (Lead Radius EXperiment) ran in Hall A in the summer and fall of 2019
- Resolved technical problems of PREX-1 (which ran in 2010)
- CREX (Calcium Radius EXperiment) ran using the same equipment in the spring and fall of 2020

	PREX-2 (^{208}Pb)	CREX (^{48}Ca)
Beam energy	0.95 GeV	2.18 GeV
Beam current	~ 70 μA	~ 150 μA
Scattering angle	4.7^0	4.5^0
Q^2	0.0062 $(GeV/c)^2$	0.0297 $(GeV/c)^2$
Rate (each HRS)	2.2 GHz	28 MHz

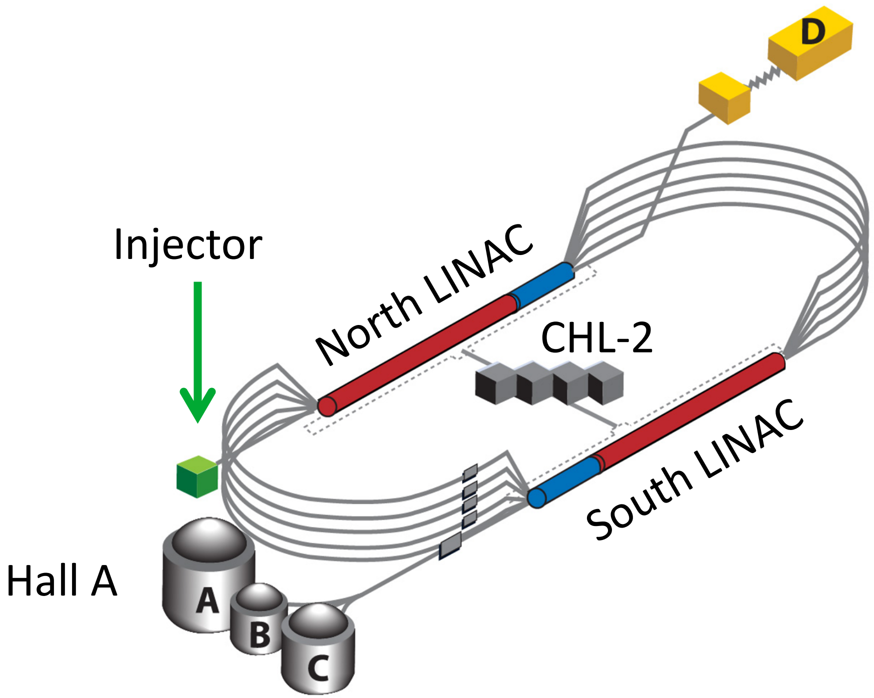

Concept of Neutron Skin ($R_n - R_p$)

Density distribution in ^{208}Pb nucleus

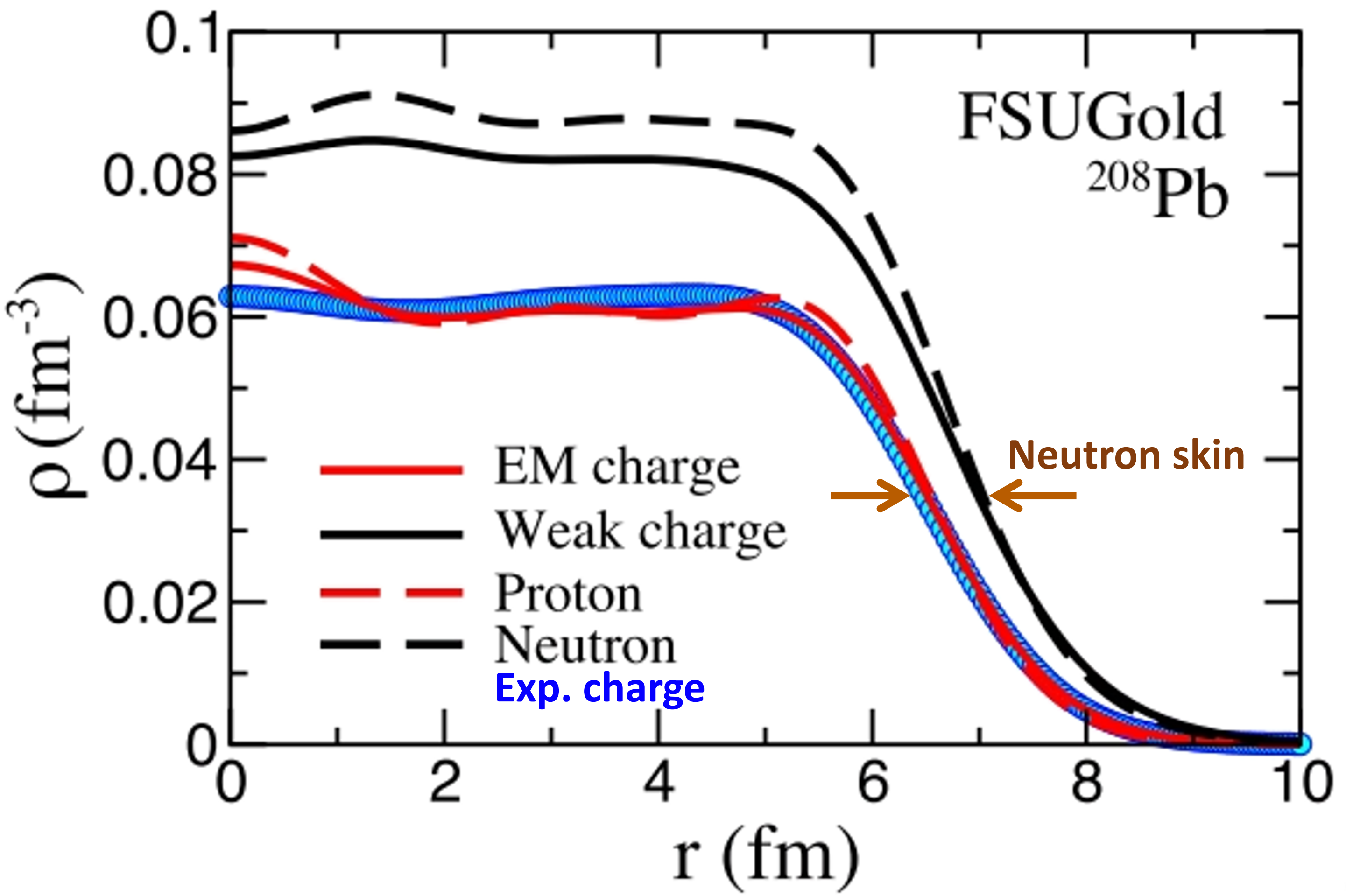

Thiel et. al. J. Phys. G:
Nucl. Part. Phys. **46**, 093003 (2019)

82 protons
126 neutrons

Parity Operation

- It is a mirror symmetry → inversion of spatial coordinates:

  $$P(x, y, z) \Longrightarrow P(-x, -y, -z).$$

- It is not conserved in weak interactions.
- Parity operation is same as changing helicity.
- **We change electron's helicity to mimic parity operation.**
- **Parity-violation creates tiny asymmetry (A_{PV}) in the detected flux.**

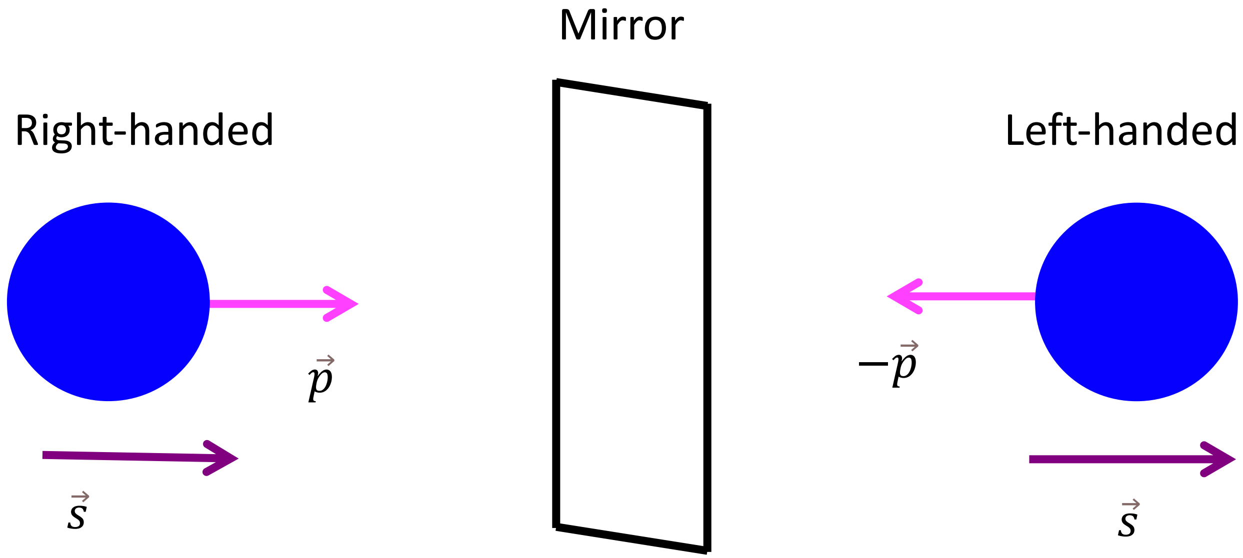

$h = \vec{s} \cdot \hat{p} \ = +s$

Parity operation

$h = \vec{s} \cdot (-\hat{p}) \ = -s$

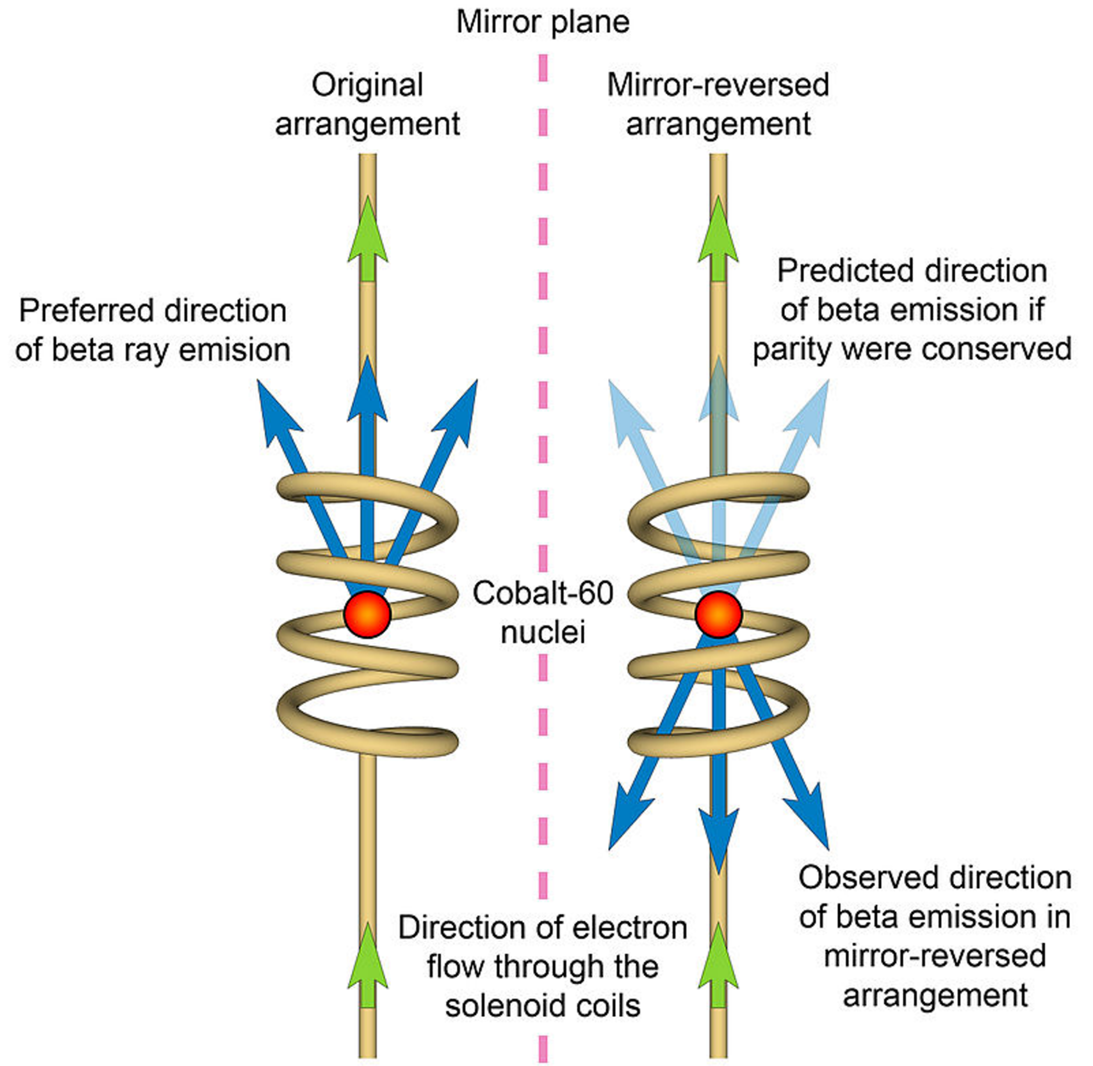

Wu Experiment (1956)

Parity-Violating Asymmetry (A_{PV})

- Elastic scattering of longitudinally polarized electrons from unpolarized (isotopically pure) targets.
- Asymmetry of the detected rates between the beam's opposite helicity states.

$$A_{PV} = \frac{\sigma_R - \sigma_L}{\sigma_R + \sigma_L} \text{ where } \sigma \sim \left|\mathcal{M}_\gamma + \mathcal{M}_{Z^0}\right|^2 \Rightarrow A_{PV} \approx \frac{2\mathcal{M}_\gamma (\mathcal{M}_{Z^0})^*}{\left|\mathcal{M}_\gamma\right|^2}$$

- For $Q^2 \ll (M_{Z^0})^2$, Born approximation gives:

0.0062 (GeV/c)^2 (91 GeV)^2

$$A_{PV} = \frac{G_F Q^2}{4\pi\alpha\sqrt{2}} \left[\underbrace{(1 - 4\sin^2\theta_W)}_{Q_W^p \approx 0.07} + \underbrace{(-1)}_{Q_W^n} \frac{F_n(Q^2)}{F_p(Q^2)} \right]$$

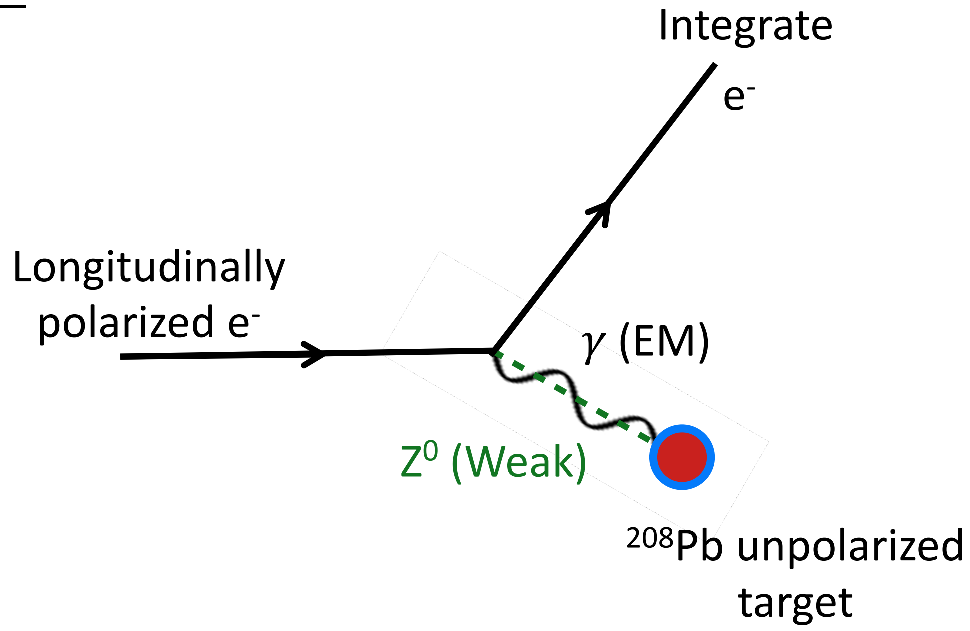

- Z^0 primarily couples with neutrons

$$A_{PV} \approx \frac{G_F Q^2 |Q_W|}{4\pi\alpha\sqrt{2}Z} \frac{F_W(Q^2)}{F_{ch}(Q^2)} \sim \left\{ \frac{10^{-4} Q^2}{(GeV/c)^2} \right\}$$

Tiny asymmetry!

Experimental Components – Polarized Source

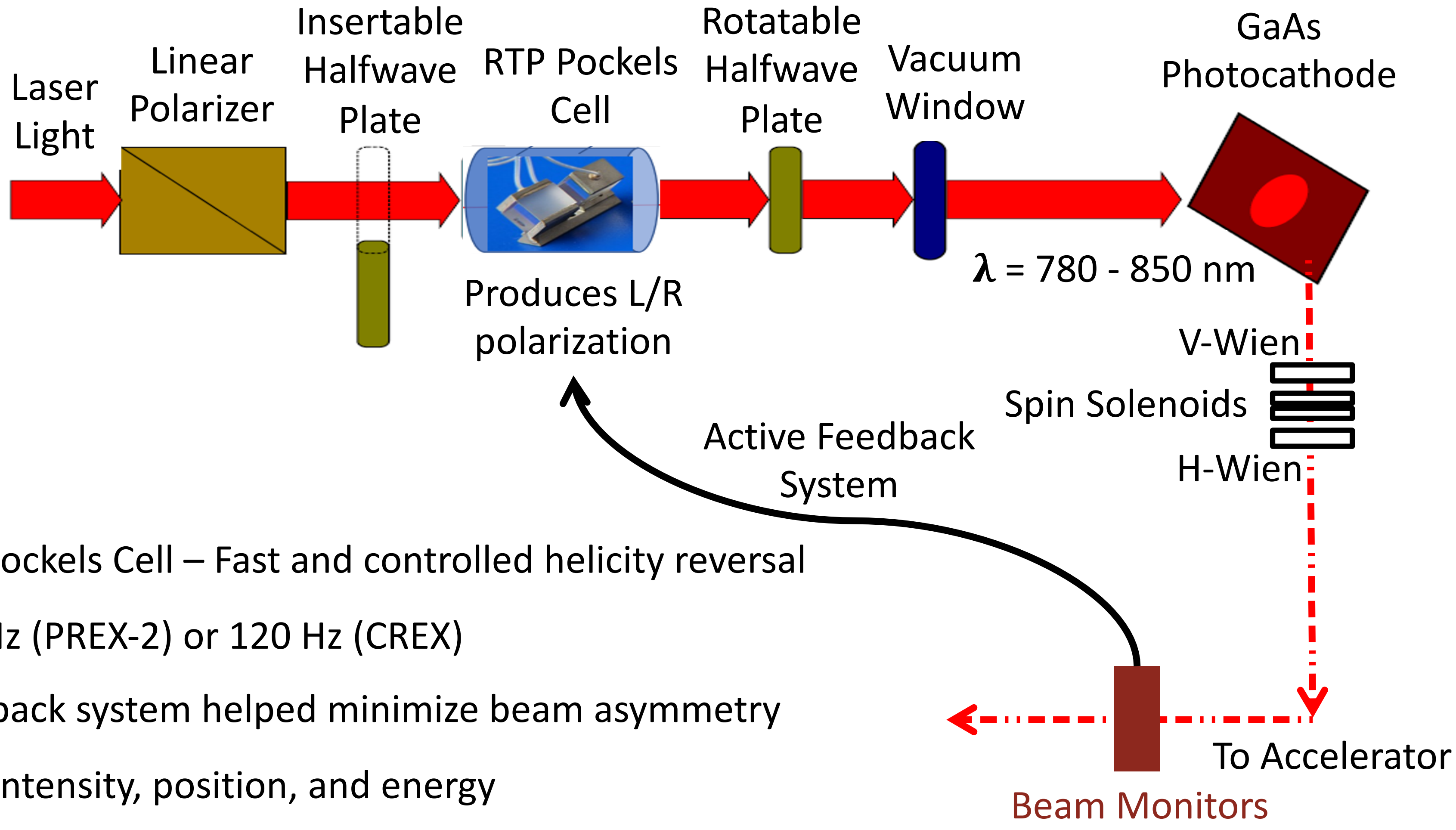

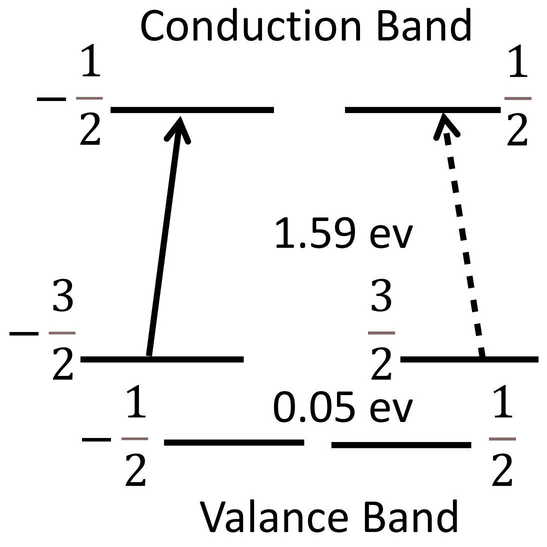

- RTP Pockels Cell – Fast and controlled helicity reversal 240 Hz (PREX-2) or 120 Hz (CREX)
- Feedback system helped minimize beam asymmetry
  - Intensity, position, and energy
- Slow helicity reversal - IHWP (~ every 8 hours)
- Double Wien rotation – electric and magnetic fields rotate electron's spin

Experimental Components – Integration Technique

- Very high rates (2.2 GHz per HRS)
  - practically impossible to count individual electrons
  - Total detected electrons → ~6×10^{15}
- Integrate detector signal over a helicity window defined by 240 Hz (or 120 Hz) flipping
- Fast helicity reversal cancels noise from
  - target density fluctuations
  - beam current fluctuations
- Pattern combination cancels 60 Hz noise associated with electronics power

$$Asym = \frac{\sum_{i=1}^{4} R_i - \sum_{i=1}^{4} L_i}{\sum_{i=1}^{4} R_i + \sum_{i=1}^{4} L_i}$$

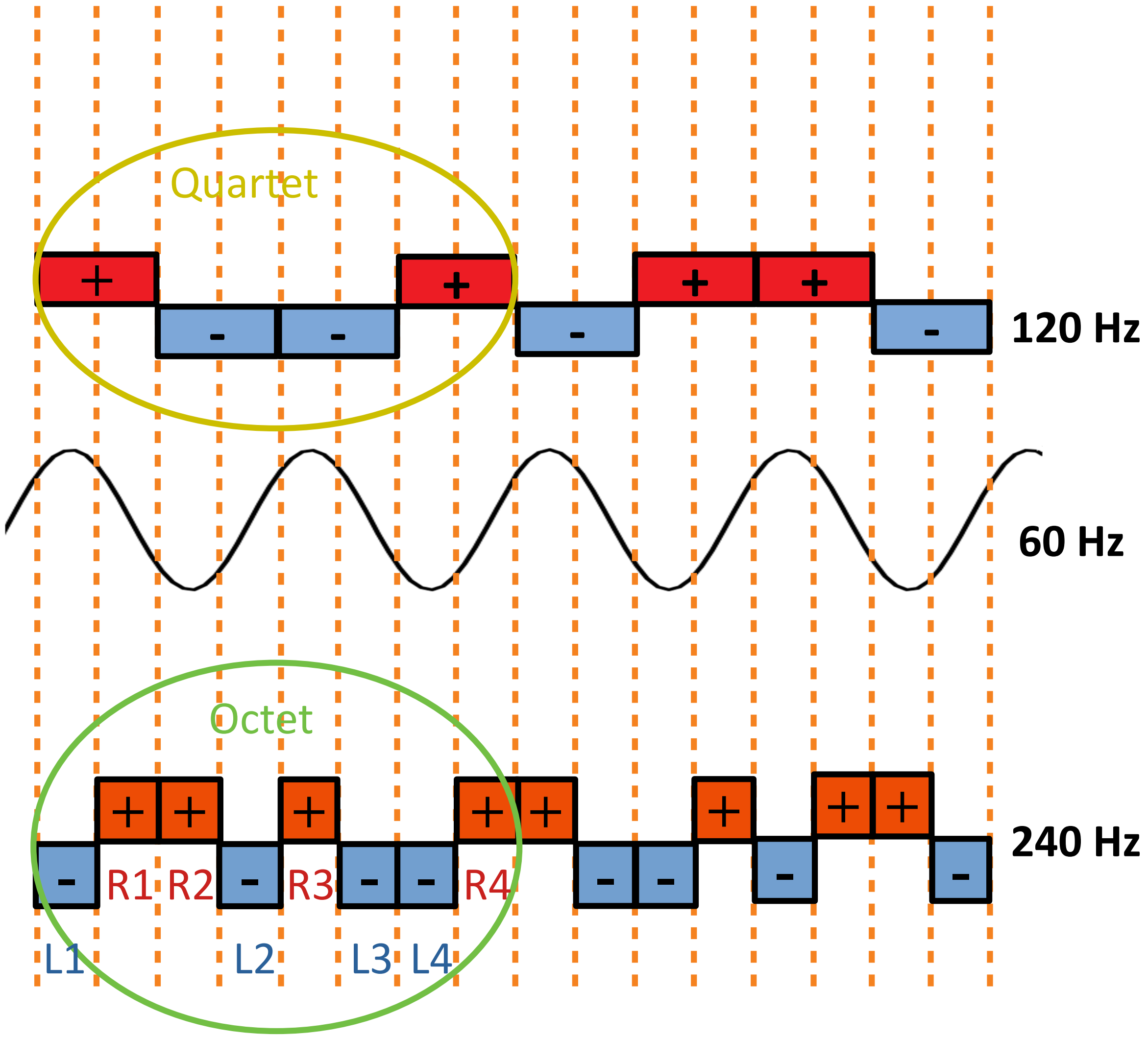

Pseudo-random helicity patterns

Experimental Components – Polarimetry

Moller polarimetry:

- Low current, invasive measurement
- Moller scattering of beam electrons from a magnetized Fe foil
- 3-4 T field gives saturated magnetization perpendicular to foil
- ~ 1 shift every 1 week
- Consistent results throughout the run

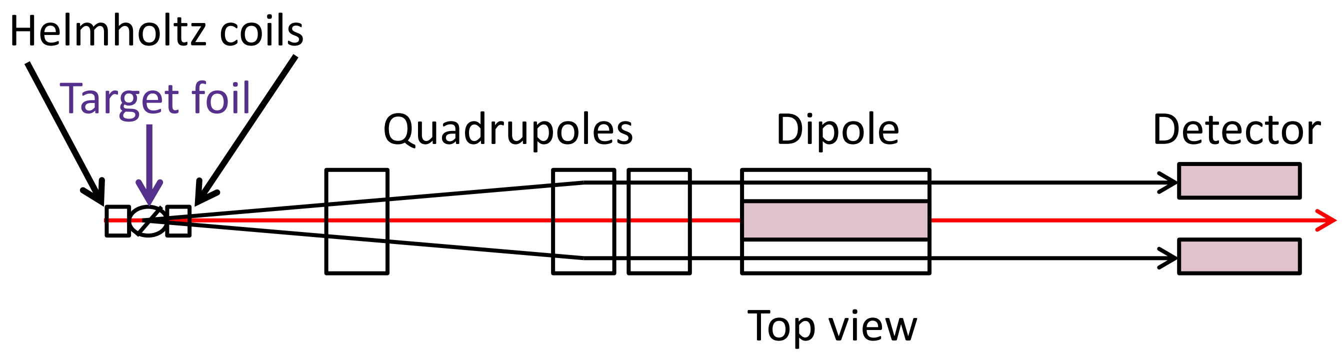

Average beam polarization for PREX-2: (89.7 ± 0.8) %

Compton polarimetry:

- Non-invasive, *in-situ*
- Challenging at low energy due to low signal and small asymmetry
- Didn't use Compton measurement for PREX-2 A_{PV} correction

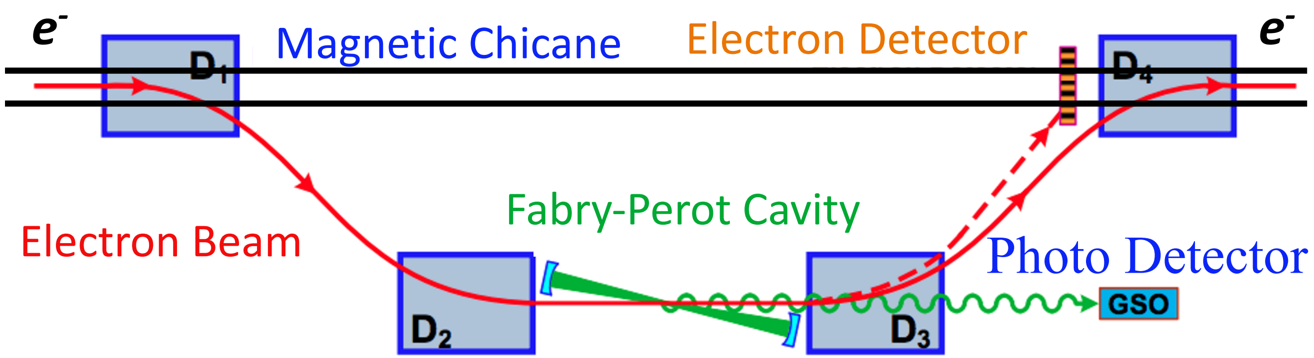

Experimental Components – Target

Production Ladder (cryo-cooled):

- 10 Diamond-^{208}Pb-Diamond targets (6 used)
- Diamond has good thermal conduction
- Diamond eventually breaks down causing damage in lead
- Target failure could be seen from increased detector width, collimator temperature, and radiation level inside the hall

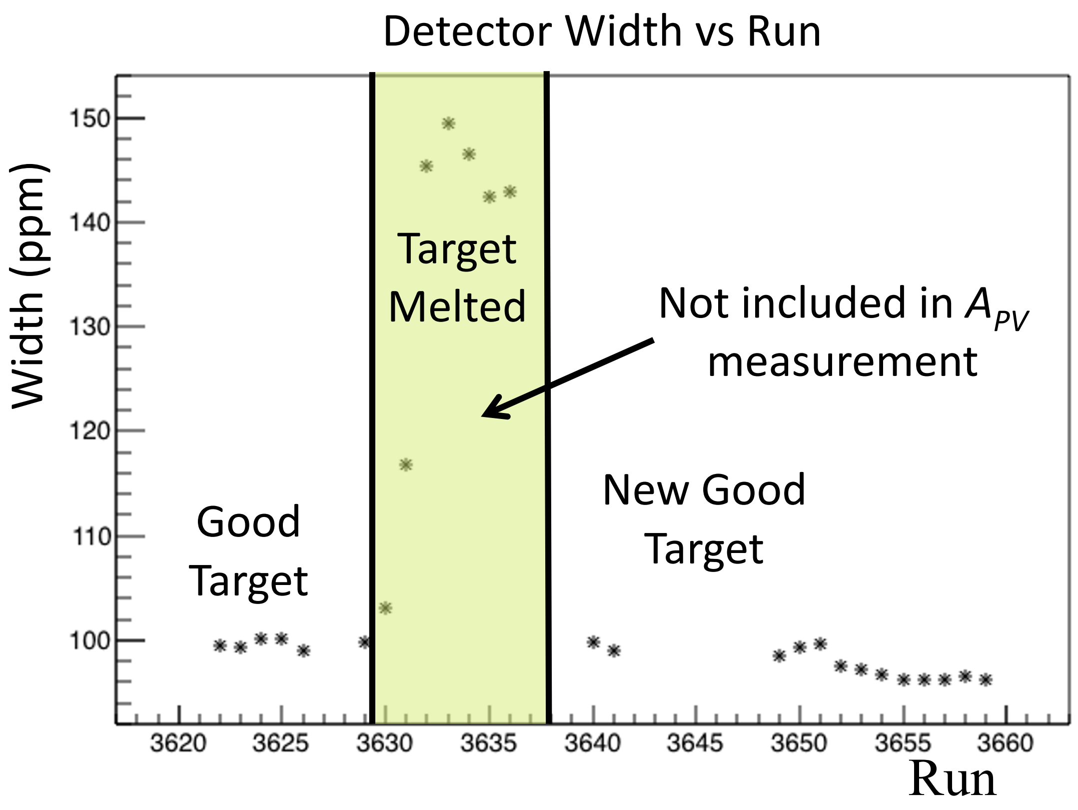

Optics Ladder (at room temperature):

- Water Cell target and Carbon-foil target
- Used for HRS optics calibration

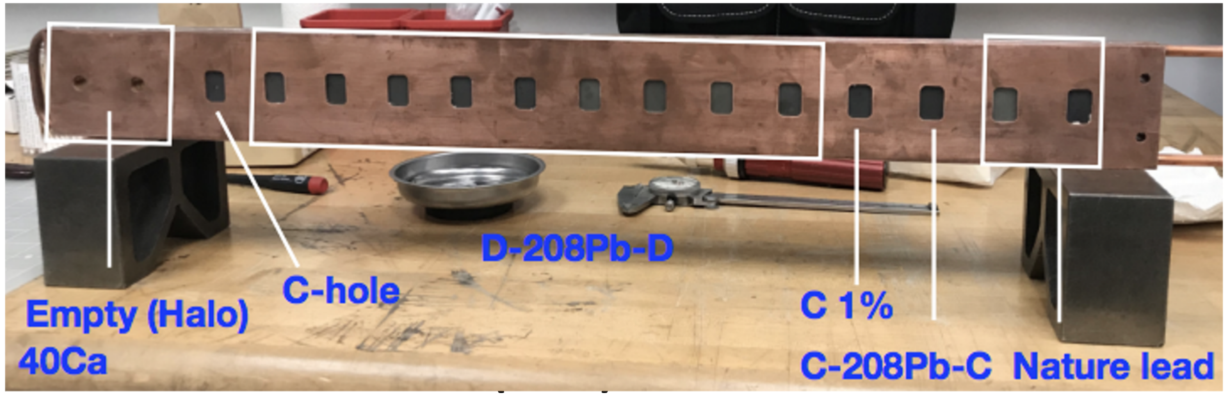

Experimental Components – HRSs

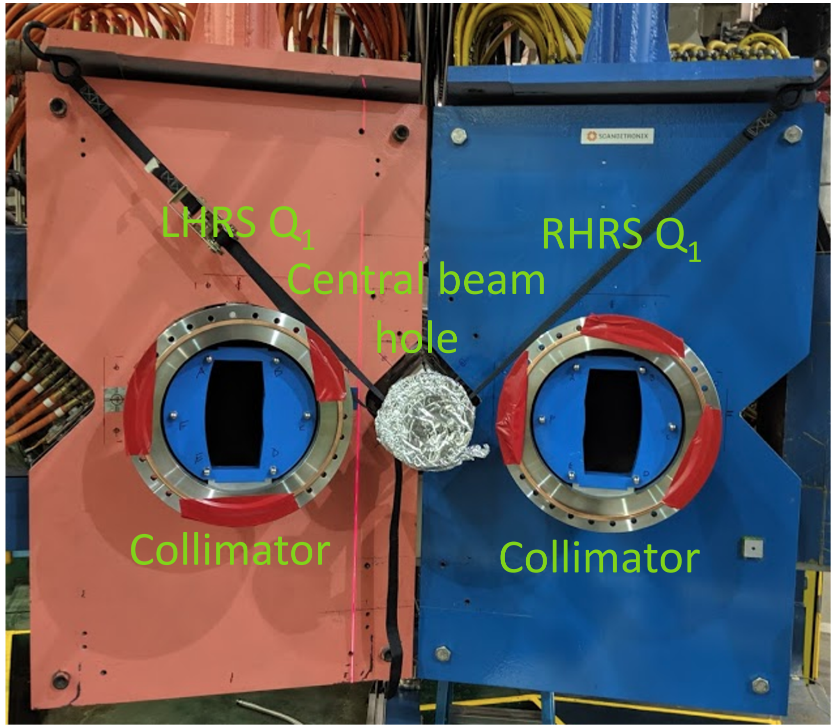

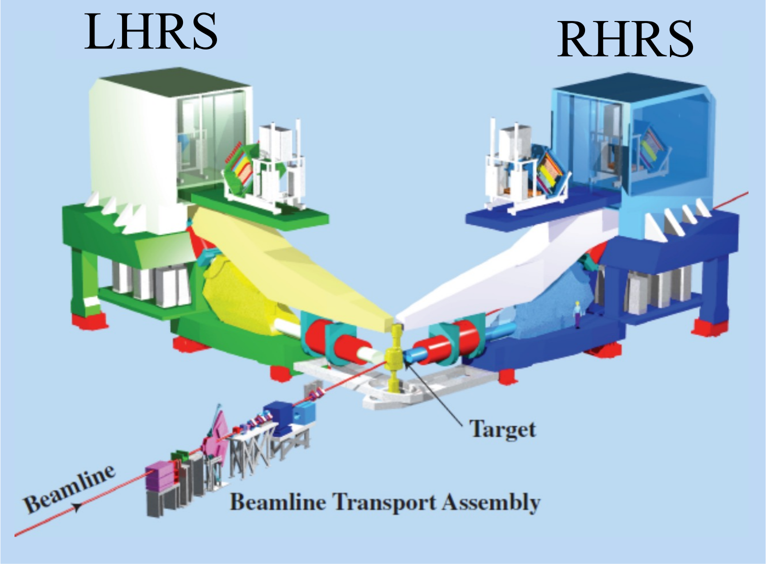

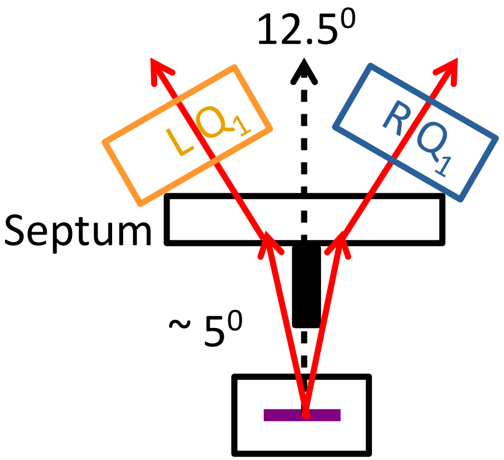

~ 600 keV hardware momentum resolution and precise detector alignment helped geometrically reject inelastic events

PREX-2/CREX Optics

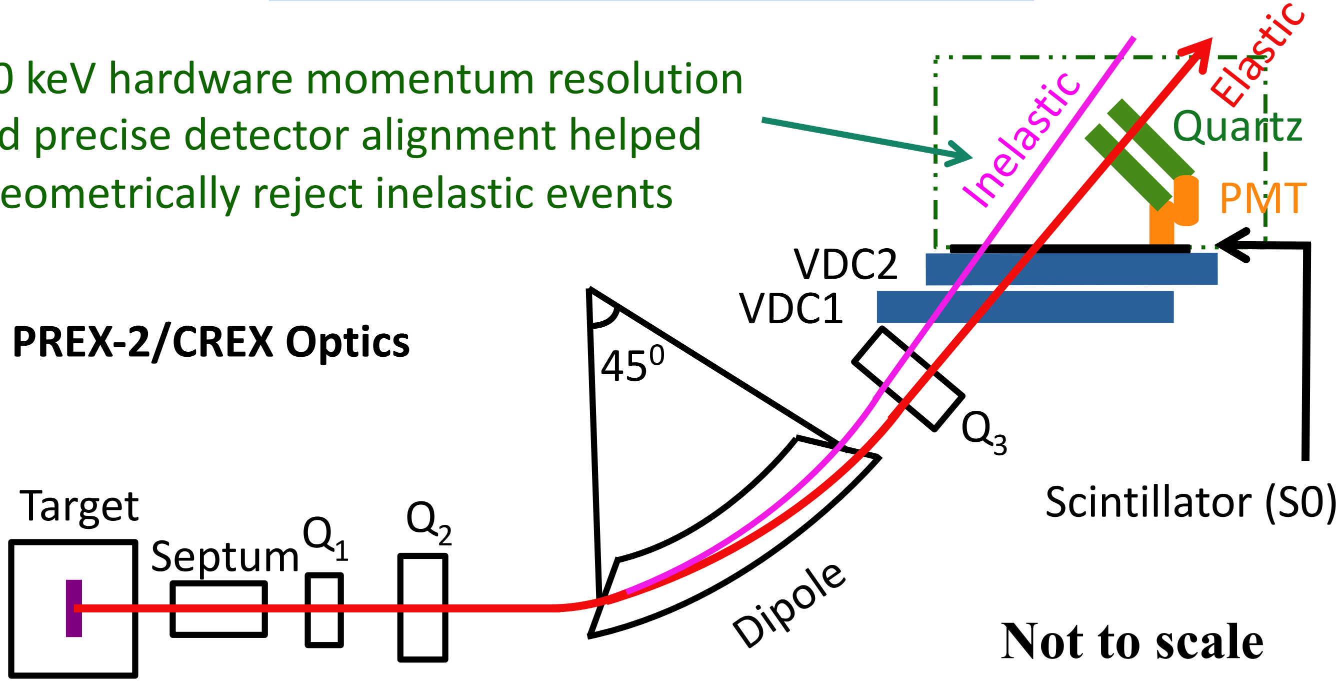

Experimental Components – Focal Plane Detectors

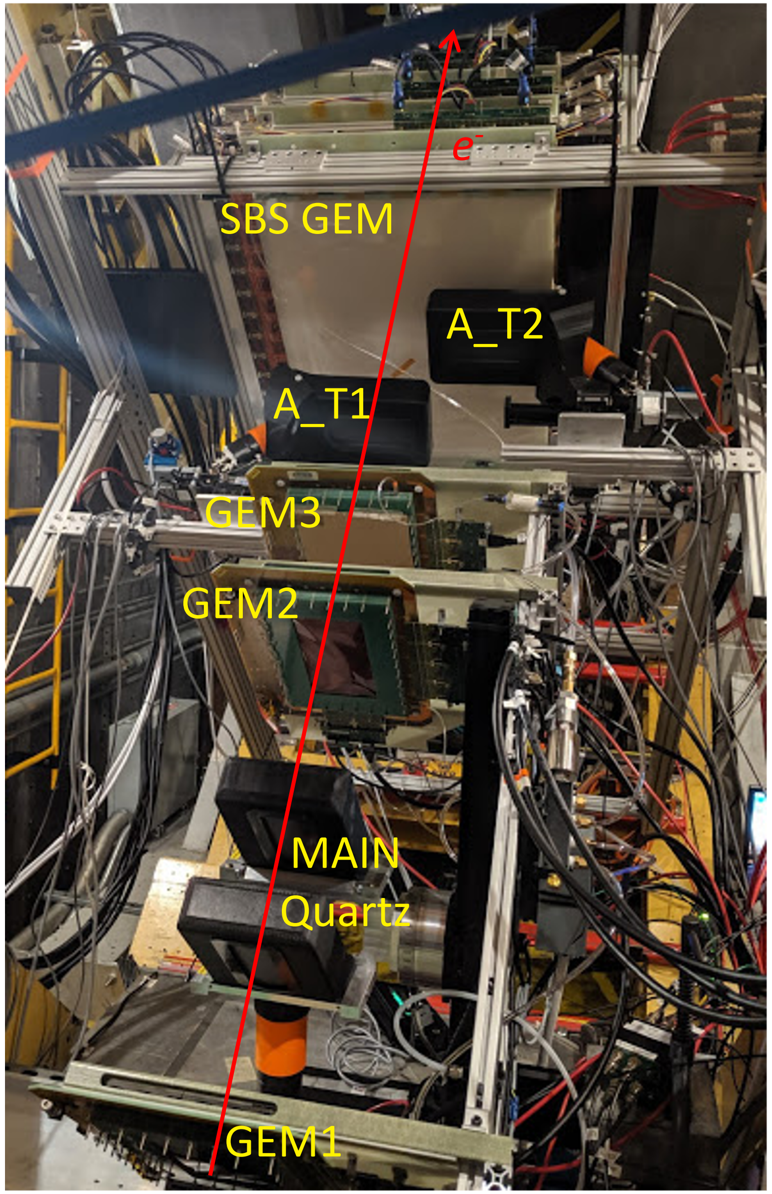

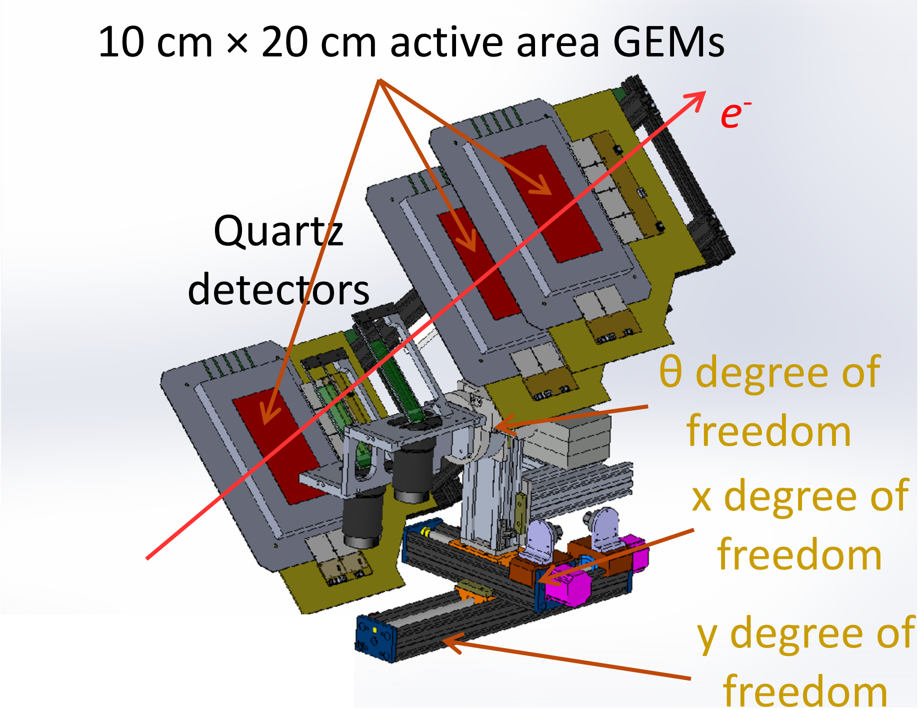

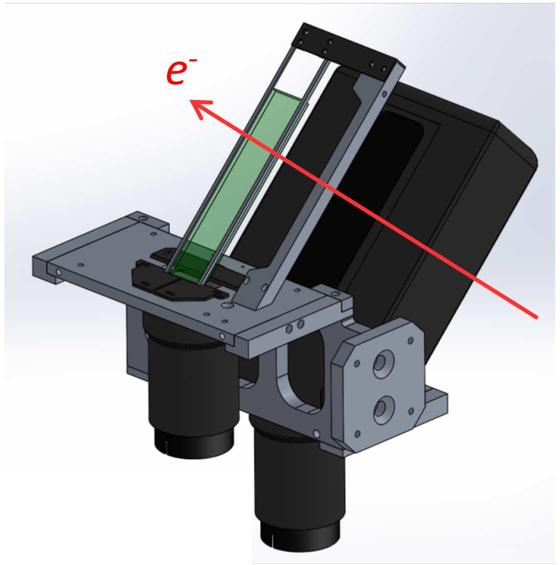

Quartz: 16cm×3.5cm×0.5cm

- Integrating detectors use rad-hard, Spectrosil 2000 fused-silica
- Tandem design is important for redundancy check and backup
- Non-linearity of detector response was tested on the bench and with beam during the experiment
- GEMs, used as backup tracking detectors – could handle orders of magnitude higher rates (~MHz/cm^2) than VDCs (10 kHz/cm^2)

Detector Alignment

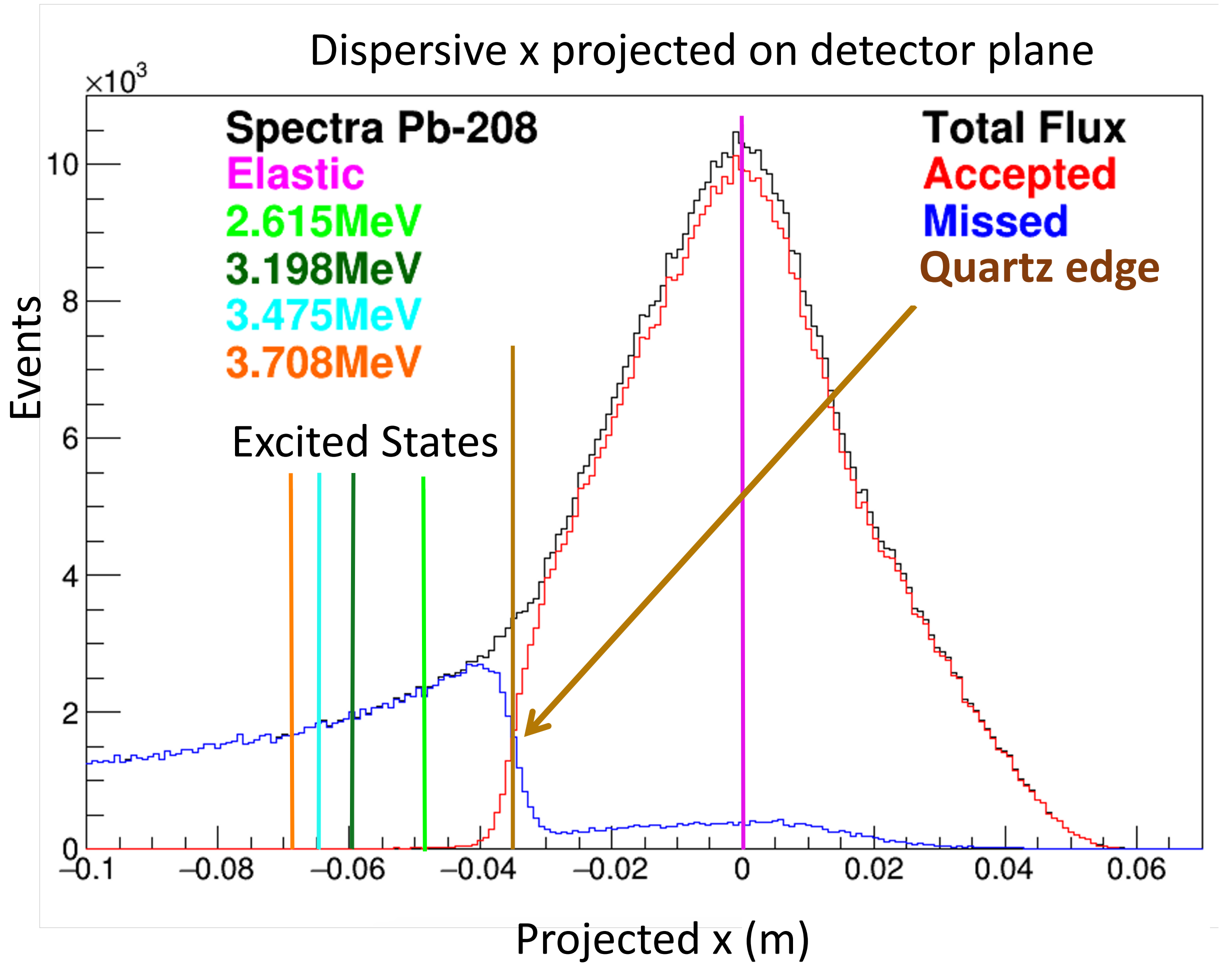

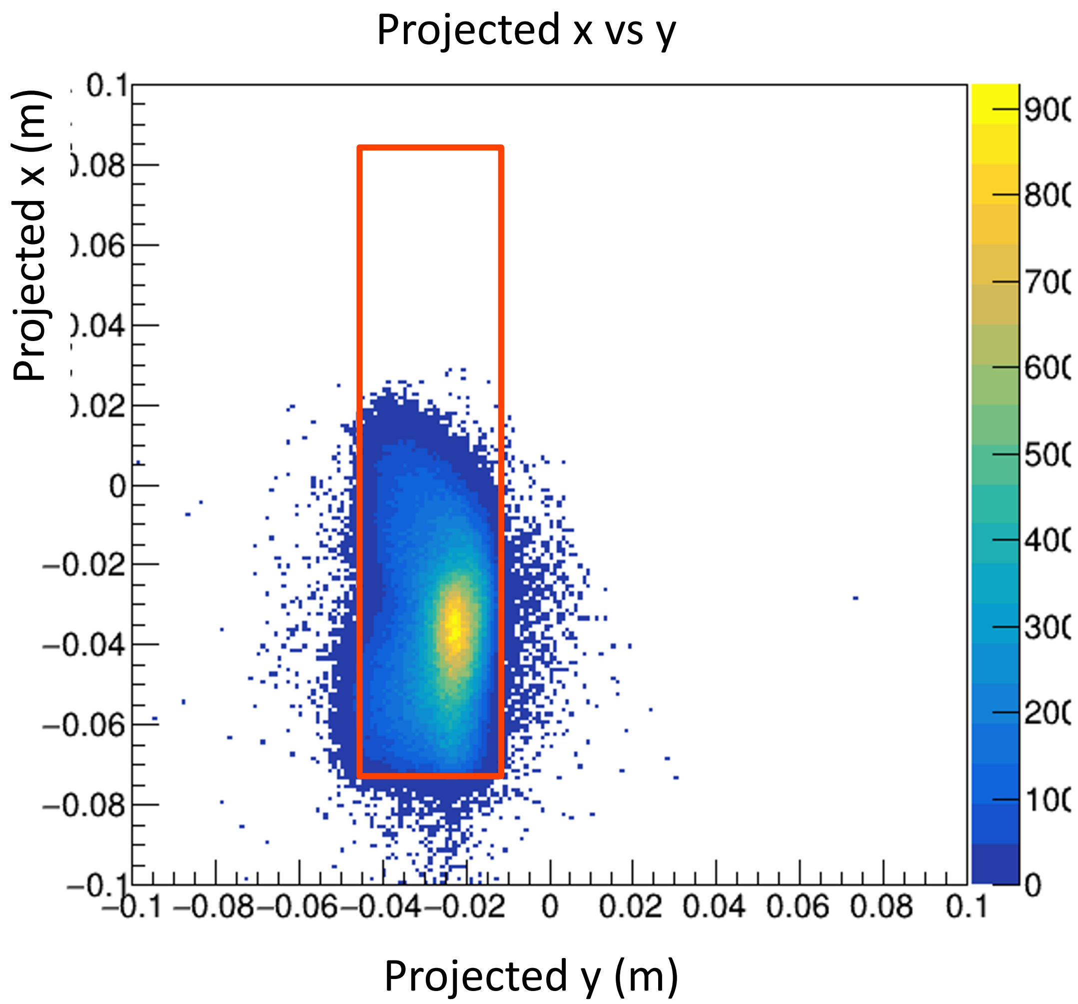

Scattering Angle Measurement & Q^2 Analysis

Energy Spectrum from Water Cell Target

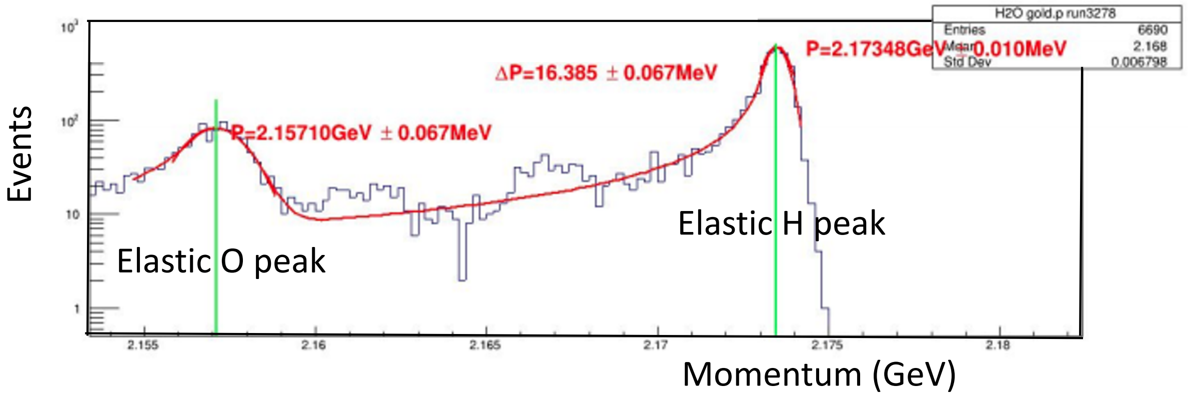

Q2 Distribution

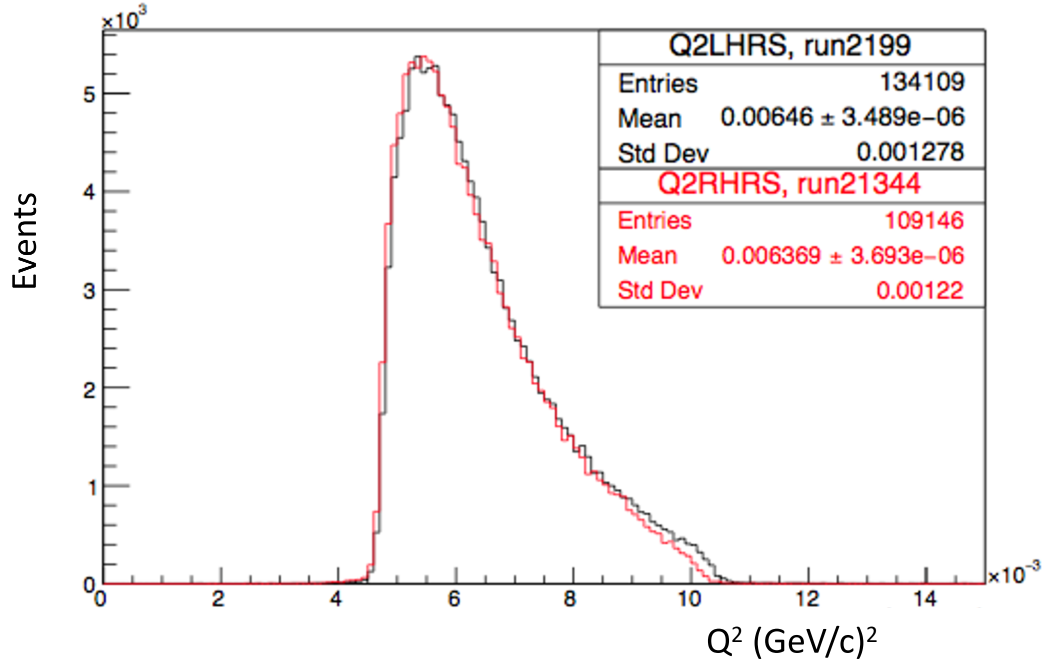

- High precision central scattering angle measurement using nuclear recoil method
- Recoil energy difference between H and O nuclei in the water cell target gives scattering angle

LHRS angle: (4.77 ± 0.02)°

RHRS angle: (4.75 ± 0.02)°

- Q2 measurements are performed periodically
- Consistent results over time

$$Q^2 = 2EE'(1-\cos\theta)$$

Q^2 average: (0.00616 ± 0.00004) (GeV/c)²

$A_{PV} \sim Q^2$

Beam Fluctuation Corrections

- Beam jitter noise is several times greater than counting statistics
- One of the major sources of systematic error
- Detector asymmetry needs proper correction for beam fluctuations:

$$A_{cor} = A_{det} - A_q - \underbrace{\left(\sum_i \alpha_i \Delta M_i + \alpha_E A_E\right)}_{A_{false}}$$

- A_{det} is the asymmetry measured by the main detectors
- Intensity asymmetry (A_q) controlled using A_q feedback system
- Total A_q correction: (20.68 ± 0.25) ppb
- Correction slopes (α_i) are calibrated using multiple techniques
  - Linear (multivariate) regression → uses natural beam motion
  - Beam modulation → uses artificial/driven beam motion
  - Lagrange multiplier → hybrid of regression and beam modulation
  - Total beam correction: $A_{false} = (-60.38 \pm 2.98)$ ppb

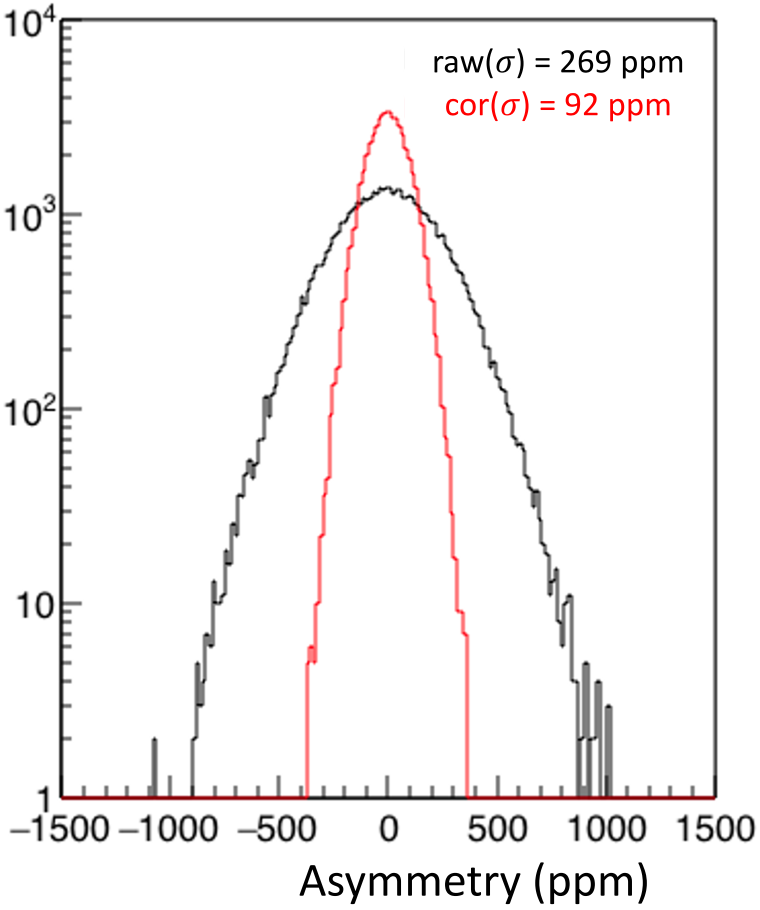

Summary of Correction and Systematic Error

Correction to A_{PV} and Systematic Uncertainty		
Source	**Absolute (ppb)**	**Relative (%)**
Polarization	56.76 ± 5.23	10.32 ± 0.95
Angle determination	0.00 ± 3.54	0.00 ± 0.64
Acceptance function	0.00 ± 2.87	0.00 ± 0.52
Beam correction	-60.38 ± 2.98	-10.98 ± 0.54
Non-linearity	0.00 ± 2.69	0.00 ± 0.49
Carbon dilution	0.69 ± 1.45	0.13 ± 0.26
Transverse asymmetry	0.00 ± 0.30	0.00 ± 0.06
Charge correction	20.68 ± 0.25	0.00 ± 0.04
Inelastic contamination	0.00 ± 0.12	0.00 ± 0.02
Rescattering	0.00 ± 0.10	0.00 ± 0.02
Total	**17.75 ± 8.16**	**3.23 ± 1.48**

$$A_{PV} = \frac{A_{cor} - P_b \sum_i f_i A_i}{P_b \left(1 - \sum_i f_i\right)}$$

A_{cor} = corrected asymmetry

P_b = beam polarization

f_i = background fraction

A_i = background asymmetry

$$A_{PV} = 550.00 \pm 16.09\,(\text{stat.}) \pm 8.16\,(\text{syst.})\ \text{ppb}$$

- Systematic uncertainties are highly controlled, statistical error is dominant

Extracting Neutron Skin (R_{skin}) from A_{PV}

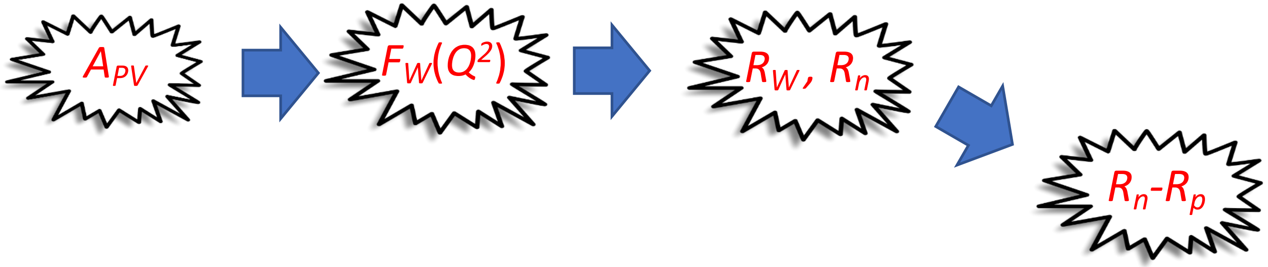

- R_W (R_{skin}) is obtained by fitting R_W (R_{skin}) against A_{PV} from various theoretical models

$$A_{PV} = 550.00 \pm 16.09\ (\text{stat.}) \pm 8.16\ (\text{syst.})\ \text{ppb}$$

$$F_W(Q^2 = 0.00616\ \text{GeV}^2) = 0.368 \pm 0.013$$

$$R_W = 5.795 \pm 0.082\ (\text{exp.}) \pm 0.013\ (\text{model})\ \text{fm}$$

$$R_{skin} = 0.278 \pm 0.078\ (\text{exp.}) \pm 0.012\ (\text{model})\ \text{fm}$$

- Combining with PREX-1 result:

$$R_{skin}^{PREX-1} = 0.30 \pm 0.18\ \text{fm}$$

C.J. Horowitz et. al.
PRC 85, 032501(R) (2012)

$$R_{skin}^{comb} = 0.283 \pm 0.071\ \text{fm}$$

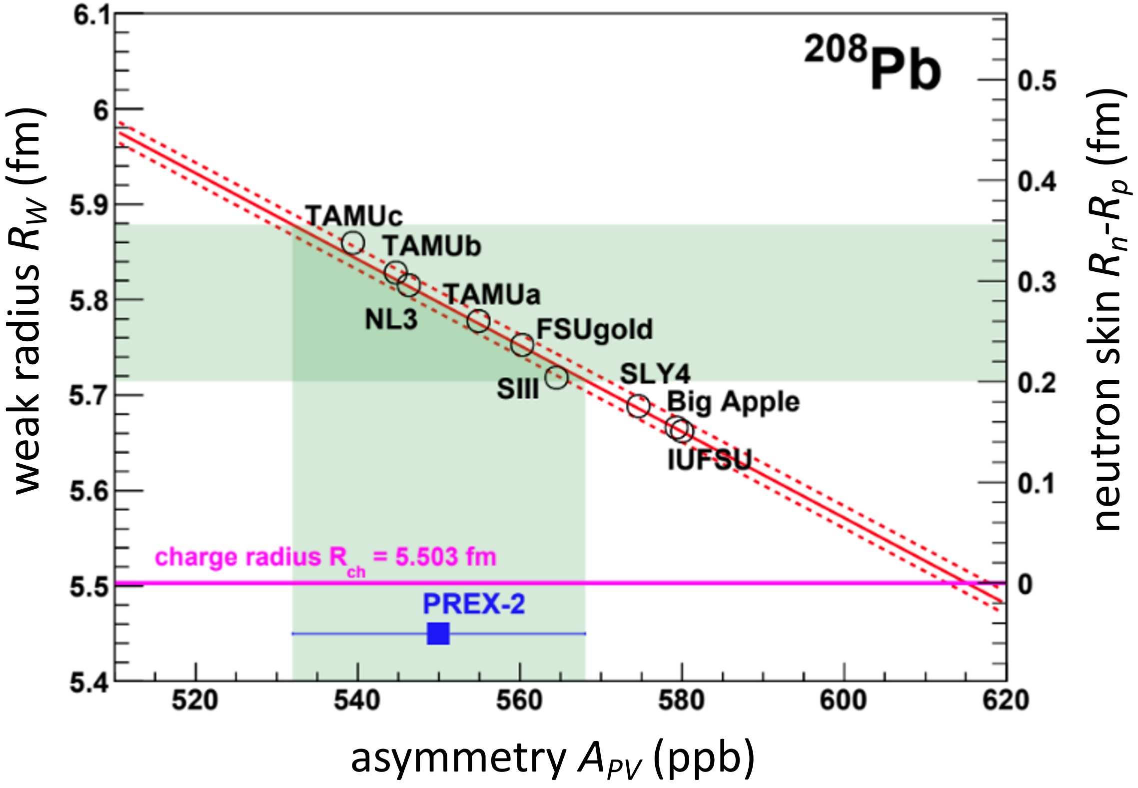

D. Adhikari et. al.
PRL 126, 172502 (2021)

Astrophysical Implication

Larger R_{skin} → Stiffer $L(\rho)$ → Greater pressure in neutron rich matter → Larger R_{NS}

$$P_{PNM}(\rho_0) \approx \frac{1}{3} L\rho_0$$

$$R_{skin}^{comb} = 0.283 \pm 0.071 \text{ fm}$$

- Implies a stiff symmetry energy $L(\rho) = \frac{dS}{d\rho}\Big|_{\rho_0}$:

$$L(\rho = \rho_0) = 106 \pm 37 \text{ MeV}$$

- $L(\rho = \rho_0)$ is closely related to the pressure of pure neutron matter
  - ➢ Suggesting larger neutron star radius (R_{NS})
  - ➢ PREX result combined with NICER suggests:

$$13.25 \leq R_*^{1.4} \text{ (km)} \leq 14.26$$

Slope Parameter $L(\rho)$ vs R_{skin} Correlation

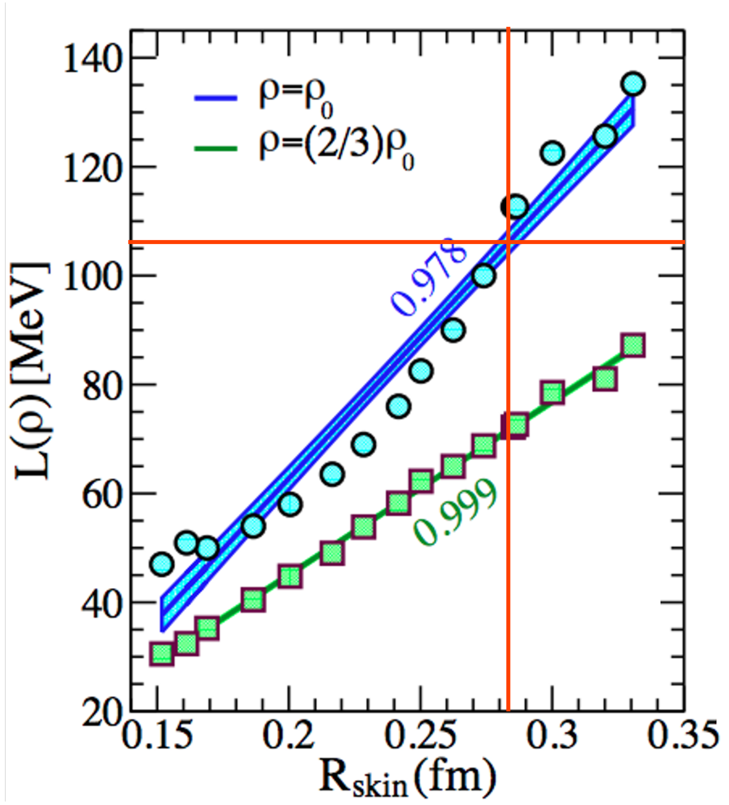

B. T. Reed et. al.
PRL 126, 172503 (2021)

A Precise Determination of Baryon Density

- Interior weak density

$$\rho_W^0 = -0.0796 \pm 0.0038\ \text{fm}^{-1}$$

- Interior charge density known

$$\rho_{ch}^0 = 0.06246\ \text{fm}^{-1}$$

- Interior baryon density

$$\rho_b^0 = \frac{1}{q_n}\rho_W^0 + \left(1 - \frac{q_p}{q_n}\right)\rho_{ch}^0$$

$$\rho_b^0 = 0.1480 \pm 0.0038\ \text{fm}^{-1}$$

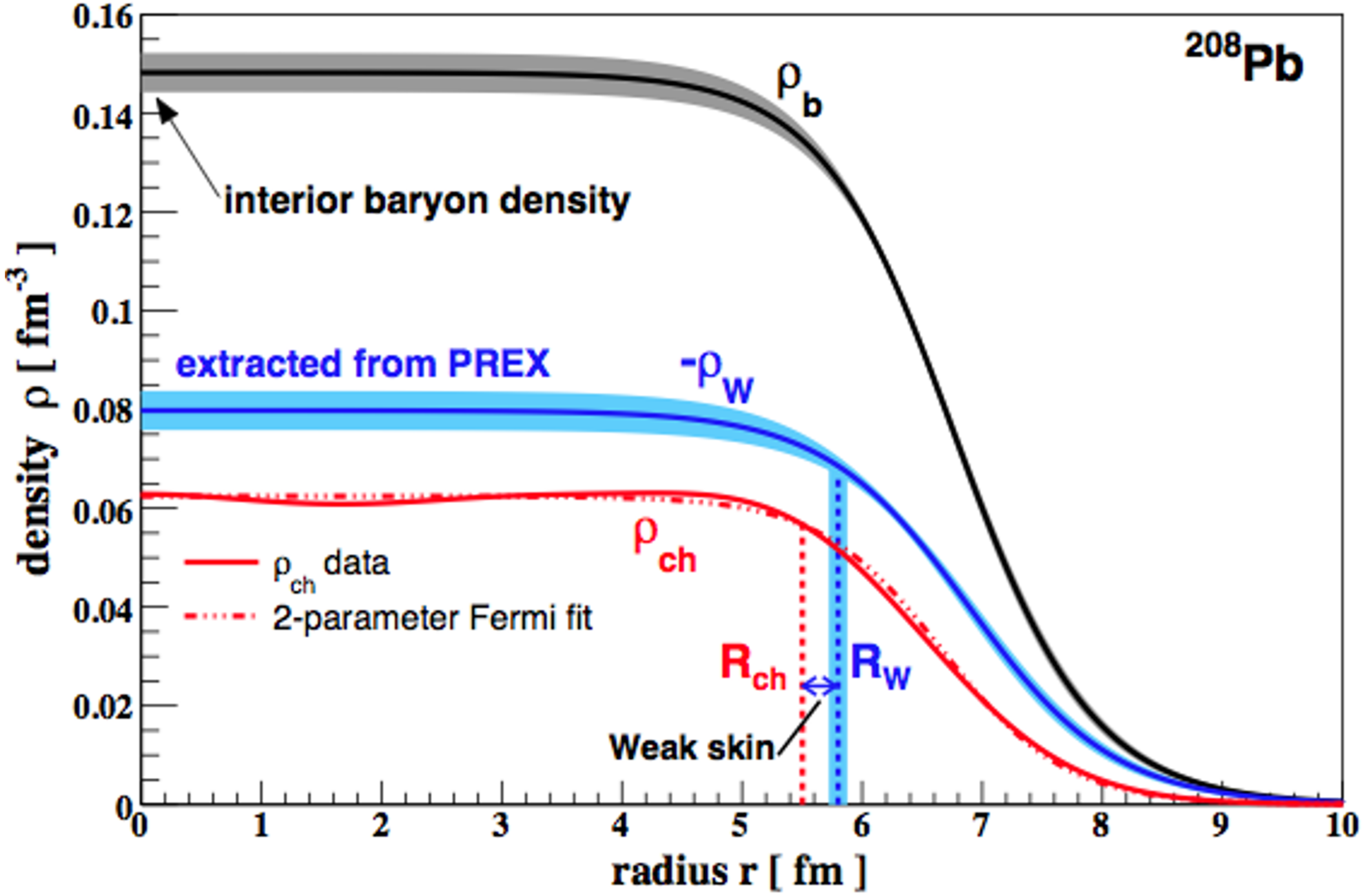

D. Adhikari et. al.
PRL 126, 172502 (2021)

Summary

- PREX-2 successfully measured neutron skin of ^{208}Pb in the Hall A and reproduced PREX-1 results (within error bar) with improved uncertainty
- Very good control over systematic → Error is statistics dominated
- A_{PV} = 550.00 ± 16.09 (stat.) ± 8.16 (syst.) ppb
- This implies neutron skin thickness for ^{208}Pb:

$$R_{skin} = 0.278 \pm 0.078\ (\text{exp.}) \pm 0.012\ (\text{model})\ \text{fm}$$

- Combining new result with PREX-1 (from 2010) gives:

$$R_{skin}^{comb} = 0.283 \pm 0.071\ \text{fm}$$

- Implies stiff symmetry energy $L(\rho=\rho_0)$ = 106 ± 37 MeV, suggesting larger possible neutron star radius
- The results have been published last year (PRL 126, 172502 (2021))
- Auxiliary (transverse asymmetry) measurements have been published recently (PRL 128, 142501 (2022))
- CREX took data following PREX-2
  - ➢ Analysis is complete and the results have been submitted to PRL publication

PREX-2 Collaboration

Students: Devi Adhikari, Devaki Bhatta Pathak, Quinn Campagna, Yufan Chen, Cameron Clarke, Catherine Feldman, Iris Halilovic, Siyu Jian, Eric King , Carrington Metts, Marisa Petrusky, Amali Premathilake, Victoria Owen, Robert Radloff, Sakib Rahman, Ryan Richards, Ezekiel Wertz, Tao Ye, Adam Zec, Weibin Zhang

Post-docs and Run Coordinators: Rakitha Beminiwattha, Juan Carlos Cornejo, Mark-Macrae Dalton, Ciprian Gal, Chandan Ghosh, Donald Jones, Tyler Kutz, Hanjie Liu, Juliette Mammei, Dustin McNulty, Caryn Palatchi, Sanghwa Park, Ye Tian, Jinlong Zhang

Spokespeople: Kent Paschke (contact person), Krishna Kumar, Robert Michaels, Paul A. Souder, Guido M. Urciuoli

Hall A techs, Machine Control and other Jefferson Lab staff have been invaluable to this experiment!

Special thanks to: Charles Horowitz and Brendan Reed for theoretical interpretations

Backup

PVeS Experiments Summary

- E122 – 1st PVeS exp. (late 70's) at SLAC
- Jlab program launched in 90's
- E158 – measured PV in Møller scattering at SLAC (2007)
- Significant improvement in experimental components over time:
  - Photocathodes
  - Polarimetry
  - Cryotargets
  - Beam stability to nanometer level
  - Low noise electronics
  - Radiation-hard detectors

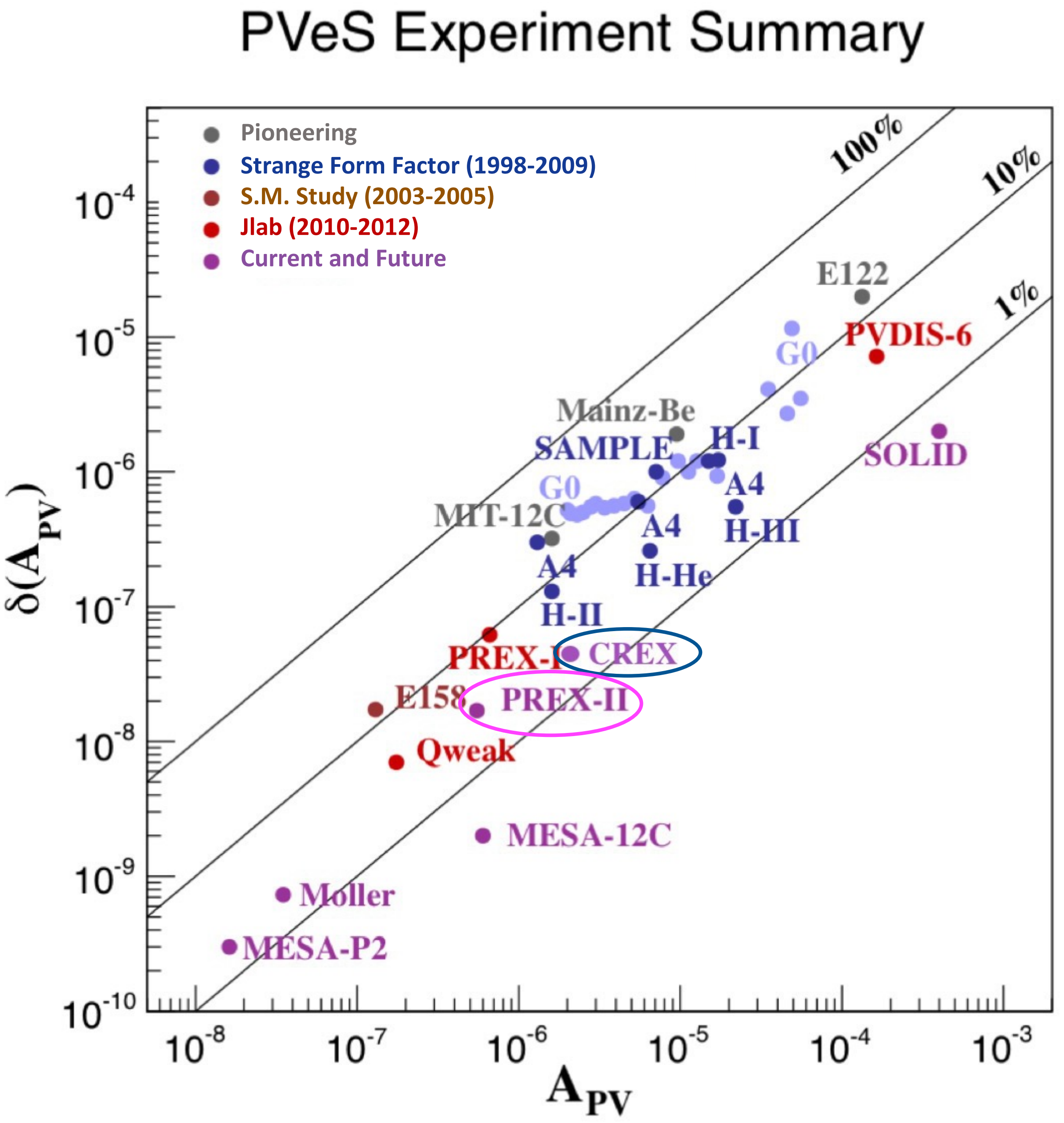

Measurement at a Single Q^2

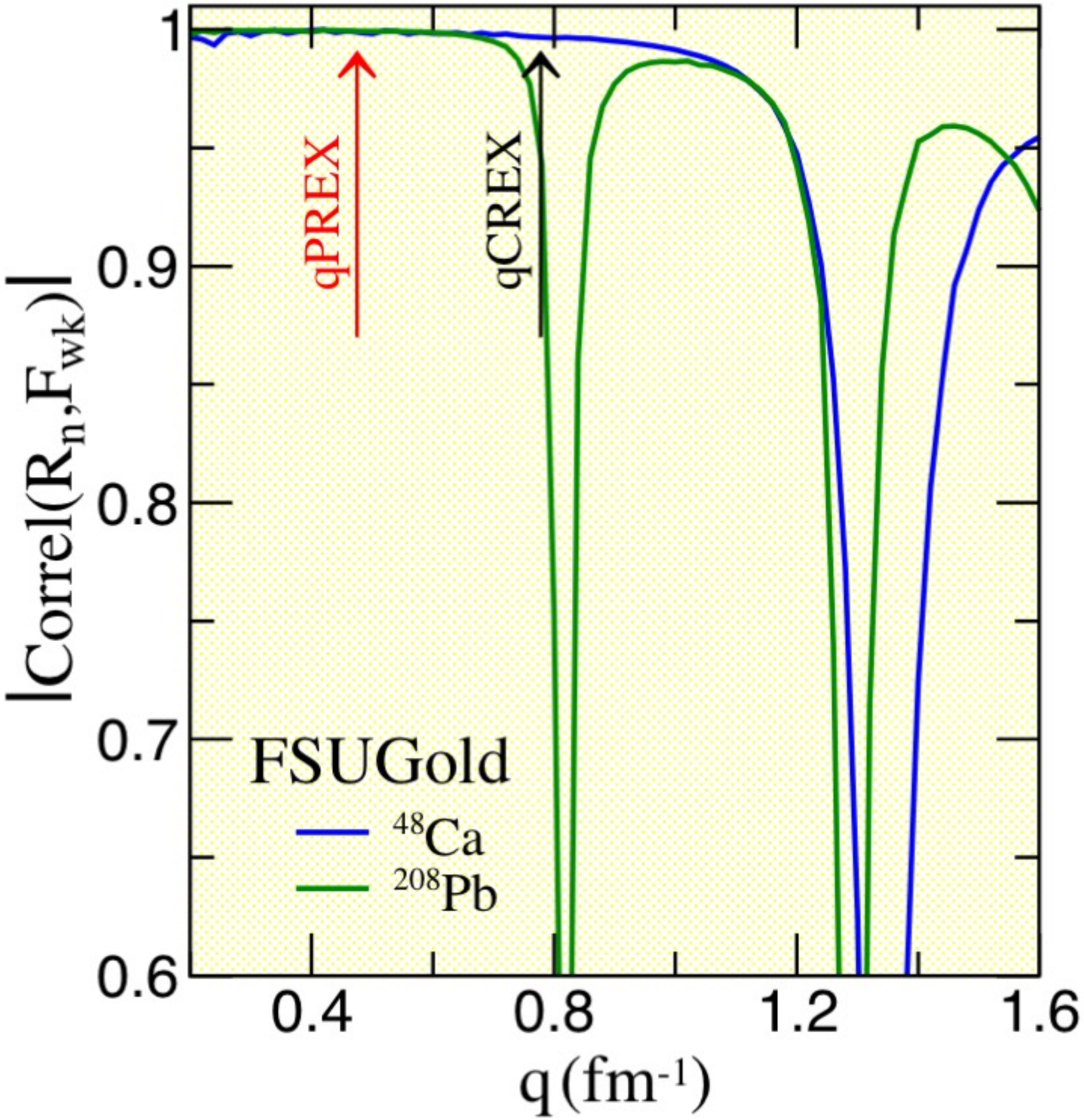

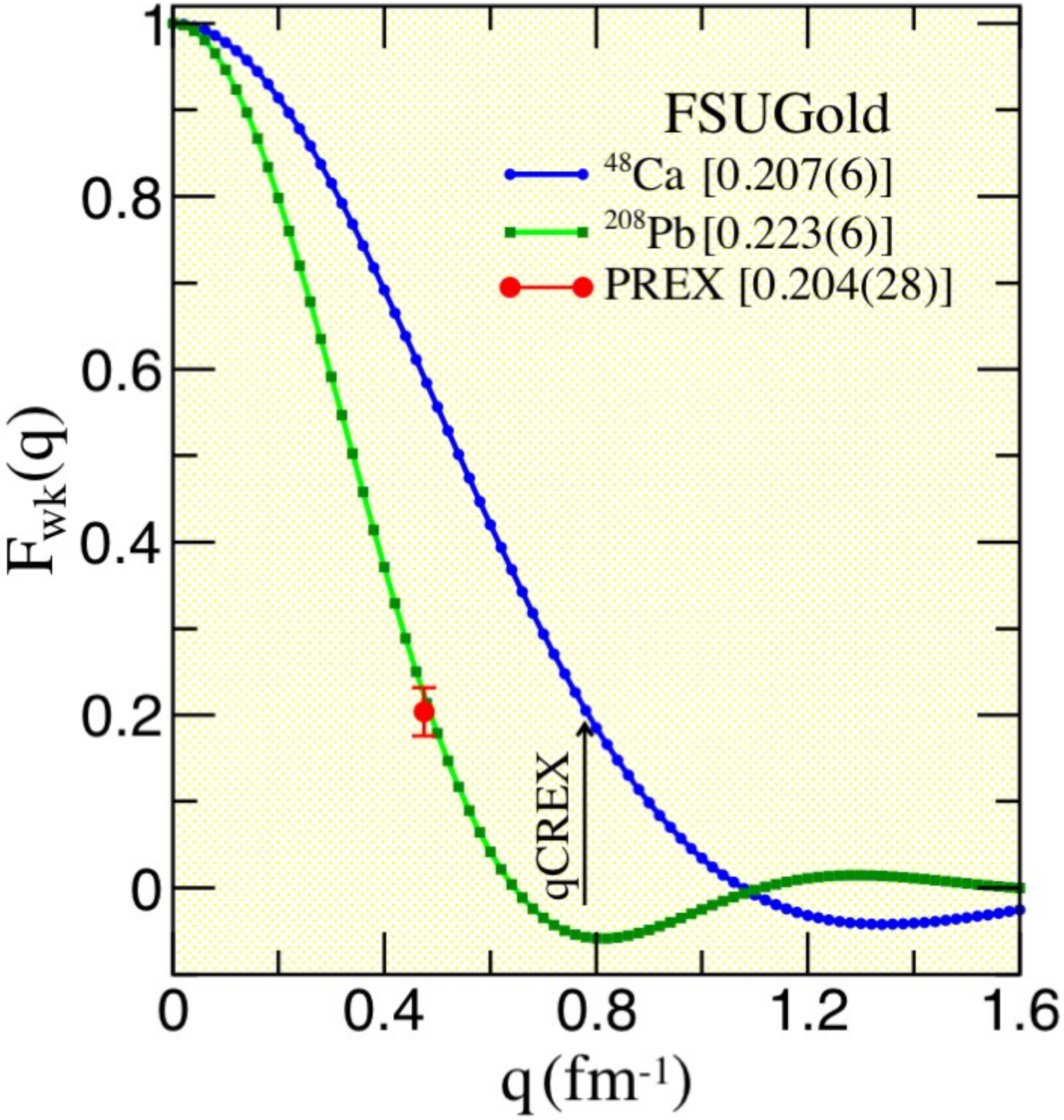

NICER vs PREX

B.T. Reed et. al.
PRL 126, 172503 (2021)

Tidal deformability (quadrupole polarizability)

$$\Lambda_*^{1.4} \sim (R_*^{1.4})^5$$

The blue band will is allowed by both PREX and NICER

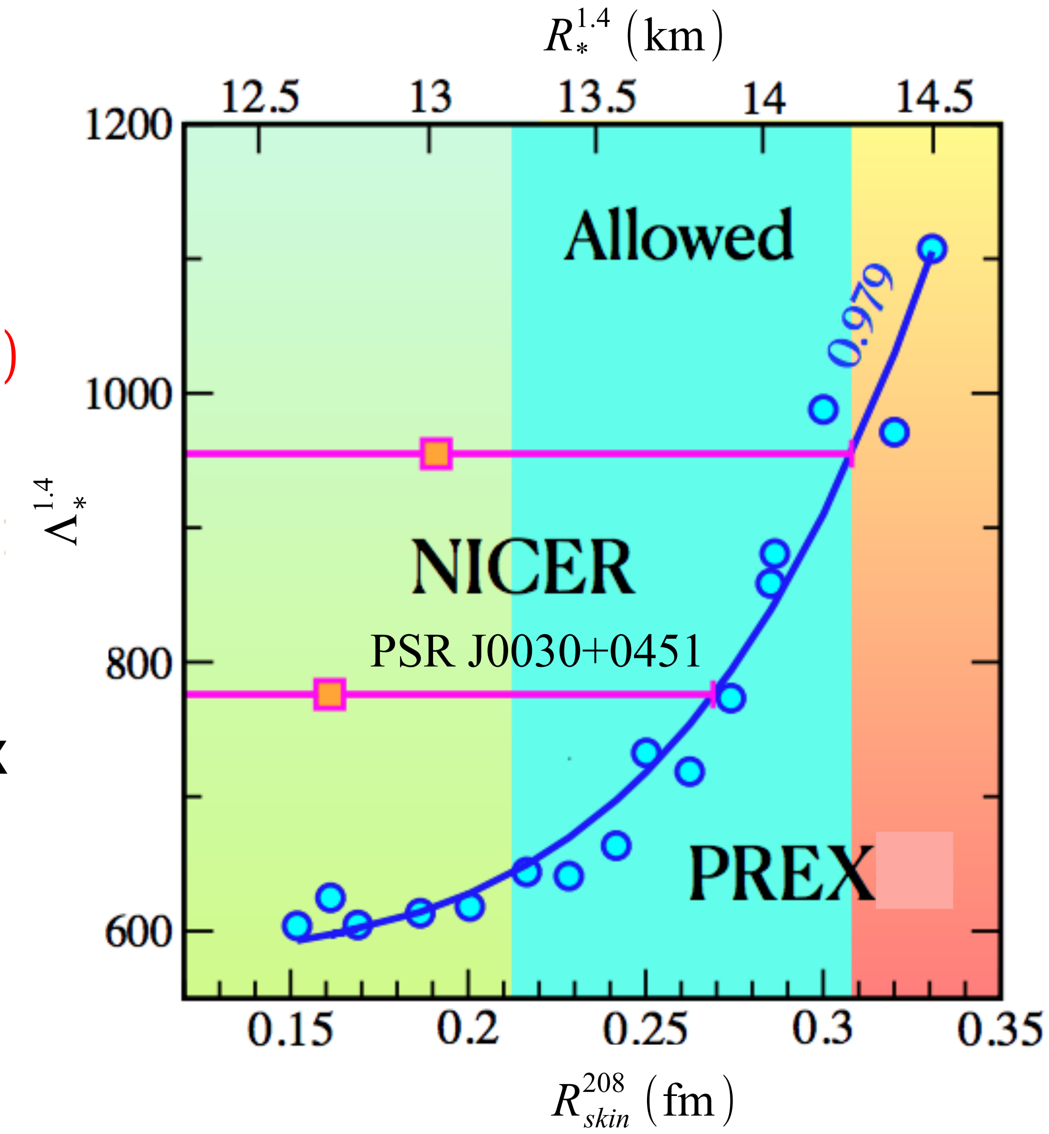

A_{PV} in Plane and Distorted Wave

Donnelly, Dubach and Sick (1988)
Horowitz, Michaels and Souder (2001)